Effects of Flame Temperature on Combustion Instabilities of a Premixed Burner

A. Okon*, A. Valera, H. Kurji, Y. Xue, R. Mash
Cardiff University, Cardiff, United Kingdom

Abstract

Combustion instabilities in gas turbine has been a major setback in the quest for efficient and clean combustion. Accurate characterisation and prediction of these disturbances is required to suppress them either at the design stage or in a close loop control when the system is in operation. The use of flame transfer functions has been a common approach in different literatures. Flame temperature is critical to the chemical time scale of the combustion system as it affects the rate of reaction. Although there has been increasing amount of literature on other factors which could modulate these instabilities, little attention has been paid to the inlet mixture – flame temperature effects on the combustion system. Thus, this study investigates these effects, using the open source acoustic simulator, (OSCILOS). Results demonstrate the temperature ratio variation as a potential method for controlling combustion instability in continuous combustion systems.

Introduction[1]

Combustion instability remains a serious challenge of continuous combustion systems such as gas turbines, especially when operated in lean premixed conditions. This is a sustained pressure oscillations in the combustion chamber caused by the coupling between the heat release fluctuations and the inherent acoustic modes of the chamber [1,2,3]. These disturbances affect the system adversely as it wears the system components and could liberate pieces into the hot gas stream to damage the downstream components in extreme cases [4,5,6].

An important condition that triggers these instabilities is that the unsteady pressure and heat release fluctuation must be in phase. The variation of this phase angle is caused by certain mechanisms and conditions, such as fuel-air ratio fluctuations, vortex shedding, flow separation, etc. The acoustic oscillation makes the equivalence ratio of the reacting mixture to vary periodically with time. This periodicity is convected to the flame with a resulting effect of heat release oscillations which drives the instability.

This coupling of the combustor acoustic with the reactive mixture is affected by the pressure drop at the injector as a result of the flow separation and rapid expansion of the flame holders. The vortex shedding in the swirling flow produces large scale coherent vortical structures [7] which are convected to the flame, resulting in the distortion of the flame front and the oscillation of heat release. These mechanisms lead to fluctuations in the time scales of the combustion system which are linked to instabilities as expressed in equation1,

$$\boldsymbol{\tau_{conv}} + \boldsymbol{\tau_{chem}} = \mathbf{KT} \qquad (1)$$

Where $\boldsymbol{\tau_{conv}}$ denotes the convective time delay, (the time required for the equivalence ratio perturbation or vortex shedding to convect from its formation point to the center of mass of the flame) and $\boldsymbol{\tau_{chem}}$ denotes the chemical time delay, while T and K denote acoustic period and a constant related to the combustor chamber acoustics, respectively [8].

A standard method of analysing combustion instabilities is to couple the flame behaviour with the acoustic wave model and solve for the resonant modes. The flame model is obtained in terms of a transfer function which relates the flame heat release fluctuation to the acoustic perturbation, [9,10]. Equation 2 gives the model as a measure of the flame response in terms of gain and phase shift which are the function of the forcing amplitude and frequency,[11].

$$\mathrm{F}(\omega, u') = \frac{Q'/\bar{Q}}{u'/\bar{u}} = \mathrm{G}(\omega, |u'|)e^{i\varphi(\omega,|u'|)} \qquad (2)$$

Where, $Q'/\bar{Q}$ denotes the normalized heat released rate perturbation and $u'/\bar{u}$, the normalised inlet velocity fluctuation that impinges on the flame front. Expressed in the frequency domain, the real part$(\omega, |u'|)$ is the gain (amplitude) and the imaginary part, $\varphi(\omega, |u'|)$ the phase of the transfer function. This transfer function is then coupled with a one - dimensional wave equation, to give a thermo-acoustic model, equation [12,13, 14] 3.

$$\frac{\mathbf{1}}{\bar{\mathbf{c}}^{\mathbf{2}}}\frac{\partial^{\mathbf{2}}\mathbf{p}'}{\partial \mathbf{t}^{\mathbf{2}}} - \frac{\partial^{\mathbf{2}}\mathbf{p}'}{\partial \mathbf{x}^{\mathbf{2}}} = \frac{\boldsymbol{\gamma}-\mathbf{1}}{\bar{\mathbf{c}}^{\mathbf{2}}}\frac{\partial \mathbf{Q}'}{\partial \mathbf{t}} \qquad (3)$$

The right-hand term gives the level of impact that the addition of heat has on the pressure disturbance. Thus with a specific heat release rate $Q'(x,t)$, the solution of the equation quantifies the resultant sound field and with the application of suitable boundary conditions, a separable solution is obtained, equation 4.

* Corresponding author: okonaa@cardiff.ac.uk

$$q'(x,t) = \text{Re}\,(\hat{p}(x)e^{i\omega t}) \quad (4)$$

This leads to an equation of the resonant frequency ω of the combustor, equation5 [15].

$$\omega^2 + 2i\omega\alpha e^{-i\omega\tau} - \omega_n^2 = 0 \quad (5)$$

When $\alpha = 0$, the roots of equation 5, are the undamped resonant organ-pipe frequency ω_n and when $\alpha \neq 0$, $\tau = 0$, the equation is solved to give

$$\omega = -i\alpha \pm (\omega_n^2 - \alpha^2)^{1/2} \quad (6)$$

which makes ω a complex term. Because the time dependence is $e^{i\omega t}$, -Im(ω) becomes the growth rate of the disturbance. Therefore,

$$e^{i\omega t} = \exp\left[\alpha t \pm i(\omega_n^2 - \alpha^2)^{1/2} t\right] \quad (7)$$

indicating that the oscillation grows exponentially if α is positive or damped if α is negative, which agrees with the Rayleigh Criterion of phase and antiphase of heat- pressure coupling. These models were scripted in Matlab by a Combustion Group at Imperial College[16, 17] and are available as an open source combustion simulator, which is used in this study.

Specific Objectives

Flame temperature is critical to the chemical time scale of the system as it affects the rate of reaction. If the initial inlet air temperature into the combustion chamber is increased, it also increases the total flame temperature in the flame zone [18]. Introducing hot air into the combustion chamber is common nowadays in many combustion processes: For instance, in order to push the blowoff limit higher in lean combustion, the inlet air is preheated. Also, Carbon Capture and Sequestration (CCS) technology, an effective means of mitigating CO_2 emission[19], selects hot CO2 from a portion of the exhaust gas and recycles it into the inlet air stream to replace nitrogen in the air and create a CO2 rich combustion atmosphere [20, 21, 22,23,24]. As shown in equation 1 this high temperature inlet mixture is going to affect the combustion instability of the system. As there are limited study in this area, this study seeks to evaluate the effects the inlet mixture – flame temperature on the instability of the system, using the Open Source Acoustic Simulator (OSCILOS). A positive outcome of this could serve as a potential technique for instability closed loop control.

Method

The combustor is captured in the user interface of the software, by loading the length and diameter of the various parts of the geometry from an external text file, figure 1. The blue section represents the inlet into the premixing chamber and the red section is the flame zone while the green section is the exit of the combustion products.

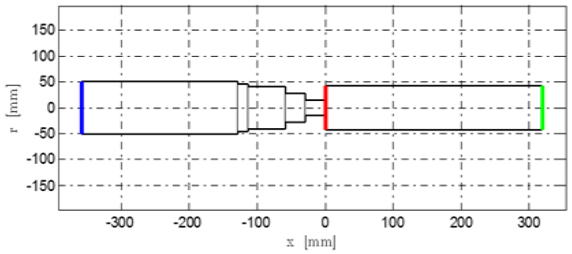

Figure 1: Combustor geometry loaded on the software interface

Table 1 presents the mean flow and thermal properties for the simulation. It uses a heating grid in place of fuel combustion, with a mean pressure P, temperature before the heating grid Tu, temperature after the heating grid Tb, mean flow velocity into the premixed chamber U1, mean flow velocity of mixture into the flame zone U2, temperature ratio Tb/Tu and mean heat release Q. Three cases were considered in this simulation, to evaluate the effects of the temperature ratio on the stability of the system.

Table 1: Flow and thermal properties of the combustor

Case	P [Pa]	Tu [K]	Tb [K]	U1 [m/s]	U2 [m/s]	Tb/Tu [-]	Q [KW]
1	101325	293.15	800	1	4.3	2.7	5.11
2	101325	293.15	1600	1	8.2	5.4	14.2
3	101325	293.15	2500	1	12.4	8.4	25.02

The flame model relates the normalised heat release rate fluctuation $Q'/\bar{Q}$ to the normalised velocity fluctuation $u'/\bar{u}$. The linear regime of the model was prescribed using an $n-\tau$ model filtered by a second order filter, where *af* is the gain, *fc*- cut-off frequency, ξ - damping ratio and τf - time delay, Table 2. The nonlinear regime was modeled based on the saturation of the heat release rate with velocity oscillation prescribed by Li et al [17], where α, β are the coefficients which shape the nonlinear regime while τn is the time delay. The boundary condition represents the link between the outward and inward propagating waves with specific coefficients for the conditions specified.

Table 2: Flame model parameters

Linear Regime				*Nonlinear Regime*			*Boundary Condition*	
af	*fc*	ξ	τf	α	β	τn	*Inlet*	*Outlet*
1.5	*250*	*0.3*	*3*	*0.8*	*25*	*3*	*choked*	*open end*

Results and Discussion

The flame oscillation is computed as presented in figure 2. The gain begins with 1.5 (for the lowest velocity ratio of 0.1) at low frequencies and rises exponentially to a peak value of 2.6 at 250Hz. The gain reduces across the velocity ratio and then saturates at 500Hz. The phase remains constant across the velocity ratio at lower frequencies but varies at higher velocity ratios. This flame behaviour was then fitted into the acoustic wave model, and the

eigenvalues (frequency, growth rate) were predicted, figure 3.

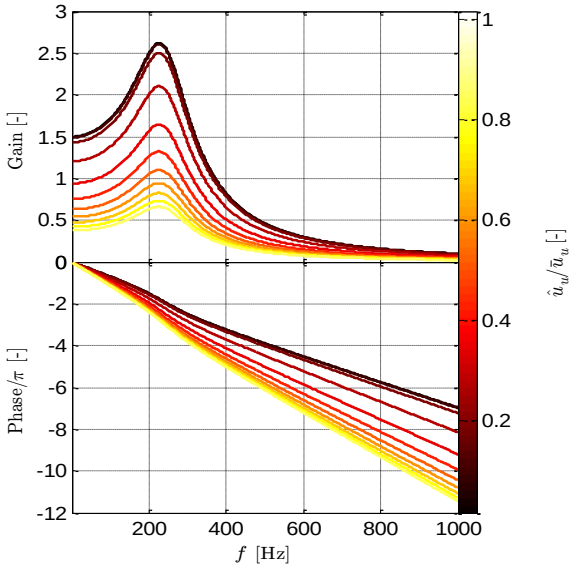

Figure2: Flame describing function computed results

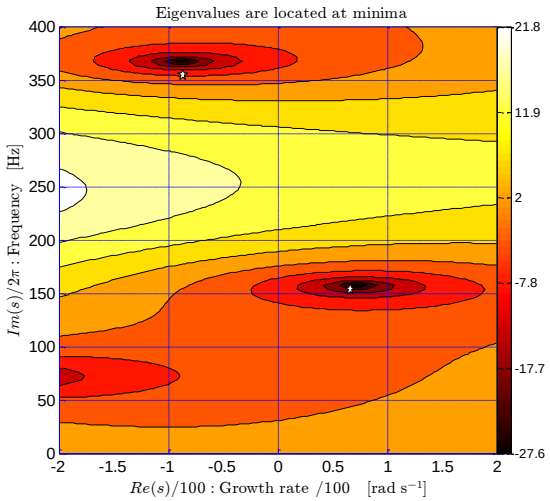

(a) $u'/\bar{u}$= 0.1

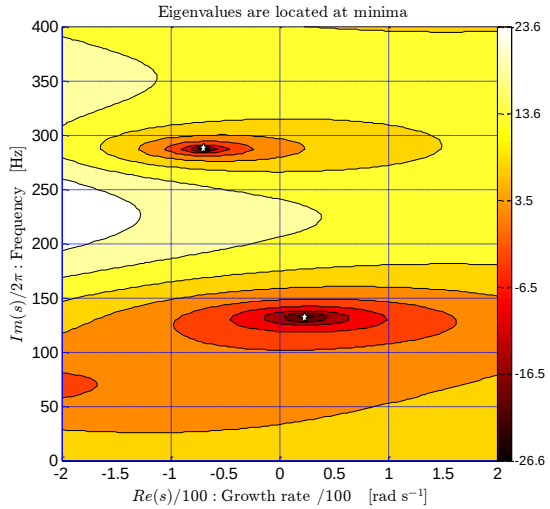

(b) $u'/\bar{u}$= 0.4

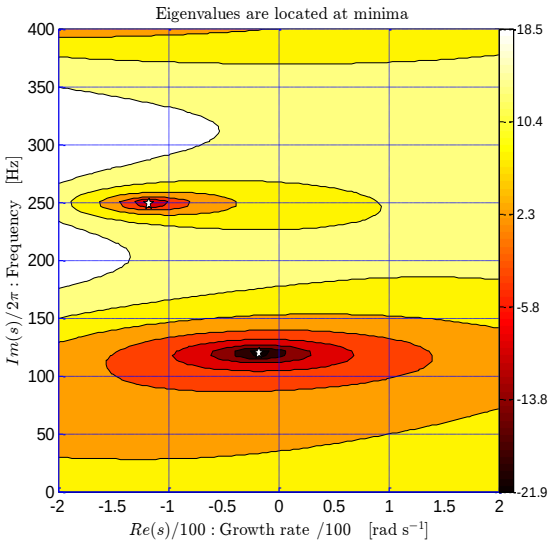

(c) $u'/\bar{u}$= 0.8

Figure 3: Contour plot of $20\log_{10}|\delta e(s)|$ in the s-plane for the normalised velocity ratios $(u'/\bar{u})$ of 0.1 (a), 0.4 (b) and 0.8 (c) of case 1.

The plots in figure 3 show two main acoustic modes designated by the white stars. As mentioned in equation 7, a positive growth rate signifies an unstable mode while a negative growth rate denotes a stable condition. This analysis focuses on the problematic unstable mode. The mode oscillates at a growth rate of 73 rad/s with a frequency of 156Hz for the velocity ratio of 0.1 for case 1, figure 3a. At a velocity ratio of 0.4, the growth rate reduces to 23 rad/s with a frequency of 131Hz, figure 3b. As the velocity ratio increases further to 0.8, the mode became stable (-17 rad/s growth rate), with a frequency of 119Hz, figure 3b. These eigenvalues were also computed for all the velocity ratios in all the three cases. The evolution of acoustic modes from an unstable state at lower velocity ratio to a stable mode at higher velocity ratio were found in all the cases, thus showing the relationship between the eigenvalues and the mixture flow velocity perturbation.

Temperature ratio variations

Figure 4a compares the evolution of the growth rate with the velocity ratios in the three cases, with the least temperature ratio in case 1 and the highest temperature ratio in case 3. In Case 1 with a temperature ratio of 2.7, the unstable acoustic mode has a growth rate of 73 rad/s at a velocity ratio of 0.1, it then reduces successively with increase in velocity ratio and reaches the limit cycle (zero growth rate) between the velocity ratio of 0.5 (8.8 rad/s) and 0.6 (-2 rad/s). In case 2 with a temperature ratio of 5.4, a realistic condition for a methane-air flame, the unsteady mode exhibits a higher growth rate of 128 rad/s at a velocity ratio of 0.1, and reduces successively till it reaches the limit cycle at 0.8 velocity ratio. In case 3, where the temperature ratio is increased further to 8.4, the growth rate of the unstable mode moves further to 148 rad/s at a velocity ratio of 0.1, and reduces with

increase in velocity ratio. However the mode still remains unstable at a velocity ratio of 0.8 and requires more increase in the velocity ratio to reach its limit cycle. It is evident that in all these cases, the growth rate decreases as the velocity ratio increases until the zero value is reached, where the flame saturates and the system becomes stable.

Figure 4b compares the evolution of the growth rate with the frequency of the unstable mode in all the cases. The frequency of the unstable acoustic mode also reduces with decrease in growth rate. In case 1, the growth rate of 73 rad/s has a frequency of 156 Hz and as the growth rate reduces to 23 rad/s, the frequency moves to 131 Hz. The mode then became stable at a rate of -17 rad/s, with a frequency of 119Hz. In case 2 with an increase in temperature ratio, the growth rate of 128 rad/s exhibits a frequency of 159 Hz for a velocity ratio of 0.1. As the rate reduces to 58 rad/s, the frequency reduces to 135Hz and reduces further to 124Hz at a growth rate of 0 rad/s. Similar trend is found in case 3 with a higher temperature ratio. Thus in all cases, the frequency decreases with decrease in growth rate. The range of growth rate and frequency increases with increase in temperature ratio from case 1 to 3.

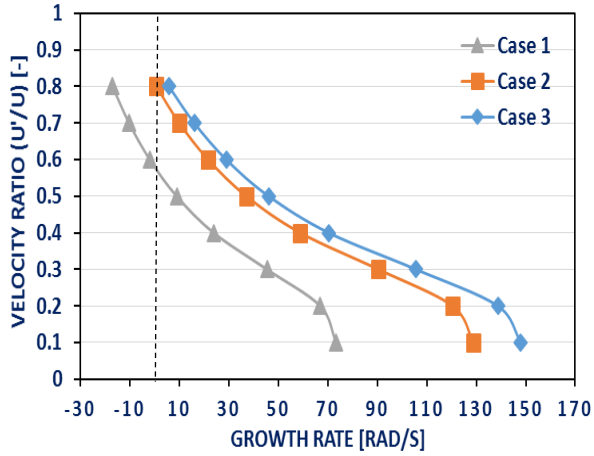

(a)

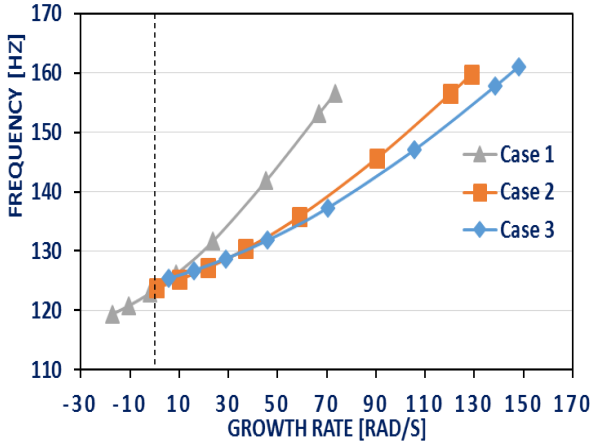

(b)

Figure 4: Eigenvalues evolution with velocity ratio for the three cases.

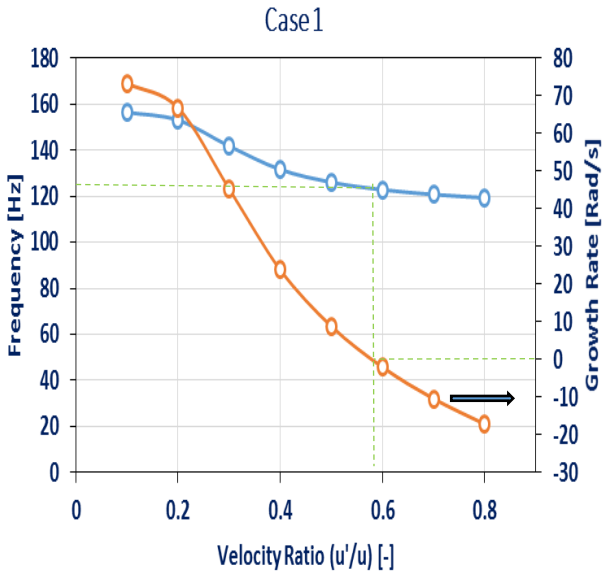

(a)

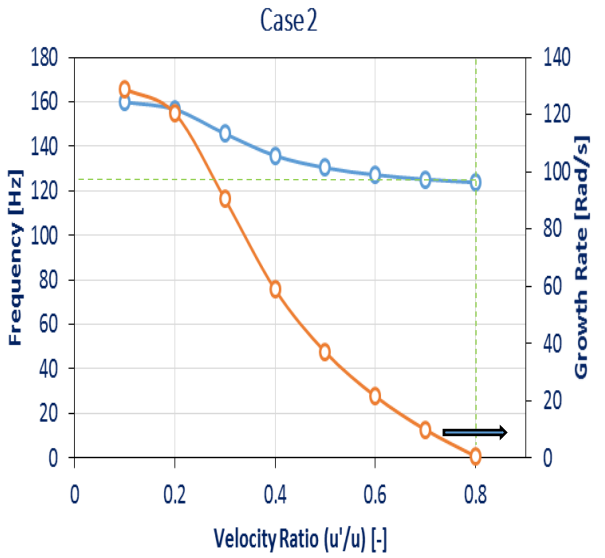

(b)

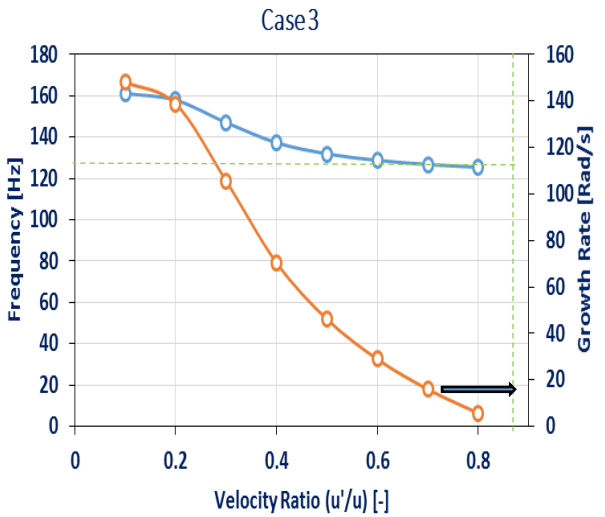

(c)

Figure 5: Limit cycle predictions of the eigenvalues

Figure 5 links the evolution of the eigen frequency and its corresponding growth rate to the velocity ratio in order to obtain the limit cycle frequency and amplitudes for the three cases. The frequency of the unstable acoustic mode (left hand side) and its corresponding growth rate (right hand side) are plotted against the eight velocity ratios (u'/u = 0.1, 0.2, 0.3, 0.4, 0.5, 0.6, 0.7 and 0.8). In case 1, figure 5a, the plot indicates that the unstable mode reaches the zero value growth rate between 0.50 and 0.60 velocity perturbations. By linear interpolation (dotted green lines), the limit cycle velocity amplitude is determined as 0.58 at a corresponding frequency of 124 Hz. Case 2, figure 5b, shows that as the temperature ratio increases to 5.4, the 124 Hz acoustic mode shifts its limit cycle amplitude to 0.8 and as the temperature ratio increases to 8.4 (Case 3), the eigen-frequency remains at 124Hz but the limit cycle velocity goes beyond the maximum 0.8 velocity perturbation (the maximum limit of this simulation) and is assumed to go as far as 0.9.

In all the three cases, even with the changes in flame temperature ratio, the limit cycle frequency remains at 124Hz but the limit cycle amplitude varies from 0.58 in case 1, 0.8 in case 2 and presumably 0.9 in case 3. It thus shows that the flame temperature could be used as an important tool to control combustion instabilities.

Table 3: Limit cycle of the eigenvalues with different temperature ratios

CASE	Temp. Ratio	Limit Cycle Frequency	Limit Cycle Amplitude
1	2.7	124	0.58
2	5.4	124	0.8
3	8.4	124	0.9 (projected)

Table 3 summarises the limit cycle values with their corresponding temperature ratios. With a constant limit cycle frequency of 124Hz, the changes in the amplitude was based on the corresponding change in temperature ratio. These results show that an unstable system could be made to reach an early limit cycle (stability) with a low velocity ratio by reducing the temperature ratio between the inlet fuel-air temperature and the temperature in the flame zone, which could be achieved by preheating the inlet air. However the temperature ratio must be kept at a value which does not reduce the overall thermal efficiency of the system. The temperature ratio variation thus becomes a potential method for the combustion instability closed loop control in continuous combustion systems.

Conclusions

The study evaluated the effects of the temperature ratio between the fuel- air inlet mixtures and flame on the instability of the system. An open source acoustic simulator which solves the coupling of the heat release fluctuation with a linear wave equation to give the eigenvalues of the acoustic modes was used. The results showed the relationship between the eigenvalues and the mixture flow velocity perturbation as the acoustic modes evolved from an unstable state at lower velocity ratio to a stable mode at higher velocity ratio. The growth rate and frequency decreased as the velocity ratio increased until the zero value growth rate (limit cycle) was reached, where the flame saturates and the system becomes stable. The range of growth rate and frequency increased with increase in temperature ratio from case 1 to 3. The limit cycle frequency remains at 124Hz in the three cases but the limit cycle amplitude varies from 0.58 in case 1, 0.8 in case 2 and presumably 0.9 (as projected) in case 3. These results show that combustion instability could be suppressed with a low flow velocity ratio by reducing the temperature ratio between the inlet mixture and the flame temperature. However, care should be taken to ensure that a high thermal efficiency is maintained with the changes in the temperature ratio. An experimental study is ongoing to validate these values.

Acknowledgements

The authors wish to thank the combustion group at Imperial College for the OSCILOS Open Source software.

References

[1] C. F. Silva, F. Nicoud, T. Schuller, D. Durox, and S. Candel, “Combining a Helmholtz solver with the flame describing function to assess combustion instability in a premixed swirled combustor,” *Combust. Flame*, vol. 160, no. 9, (2013) pp. 1743–1754.

[2] X. Han, J. Li, and A. S. Morgans, “Prediction of combustion instability limit cycle oscillations by combining flame describing function simulations with a thermoacoustic network model,” *Combust. Flame*, 162 (10) 2015 pp 3632-3647.

[3] P. Palies, D. Durox, T. Schuller, and S. Candel, “Experimental study on the effect of swirler geometry and swirl number on flame describing functions,” *Combust. Sci. Technol.*, vol. 183, no. 7, (2011) pp. 704–717.

[4] R. Balachandran, B. O. Ayoola, C. F. Kaminski, A. P. Dowling, and E. Mastorakos, “Experimental investigation of the nonlinear response of turbulent premixed flames to imposed inlet velocity oscillations,” *Combust. Flame*, vol. 143, no. 1, (2005) pp. 37–55.

[5] T. Lieuwen, H. Torres, C. Johnson, and B. T.

Zinn, “A Mechanism of Combustion Instability in Lean Premixed Gas Turbine Combustors,” *J. Eng. Gas Turbines Power*, vol. 123, no. 1, pp. 182–190, 2001.

[6] X. Han, J. Yang, and J. Mao, “LES investigation of two frequency effects on acoustically forced premixed flame,” *Fuel*, 2016.

[7] N. Syred, “A review of oscillation mechanisms and the role of the precessing vortex core (PVC) in swirl combustion systems,” *Progress in Energy and Combustion Science*. 2006.

[8] T. Lieuwen, V. McDonell, E. Petersen, and D. Santavicca, “Fuel flexibility influences on premixed combustor blowout, flashback, autoignition, and stability,” *J. Eng. gas turbines power*, vol. 130, no. 1, (2008) p. 11506.

[9] C. F. Silva, F. Nicoud, T. Schuller, D. Durox, and S. Candel, “Combining a Helmholtz solver with the flame describing function to assess combustion instability in a premixed swirled combustor,” *Combust. Flame*, vol. 160, no. 9, (2013.) pp. 1743–1754, [10]

P. Palies, D. Durox, T. Schuller, and S. Candel, “Nonlinear combustion instability analysis based on the flame describing function applied to turbulent premixed swirling flames,” *Combust. Flame*, vol. 158, no. 10, (2011) pp. 1980–1991.

[11] S. R. Stow and A. P. Dowling, “A time-domain network model for nonlinear thermoacoustic oscillations,” *J. Eng. gas turbines power*, vol. 131, no. 3, (2009) p. 31502.

[12] A. P. Dowling, “The calculation of thermoacoustic oscillations,” *J. Sound Vib.*, vol. 180, no. 4, (1995) pp. 557–581.

[13] T. Lieuwen, “Modeling Premixed Combustion–Acoustic Wave Interactions: A Review,” *J. Propuls. POWER*, vol. 19, no. 5, (2003).

[14] D. You, X. Sun, and V. Yang, “A three-dimensional linear acoustic analysis of gas turbine combustion instability,” *AIAA Pap.*, vol. 118, 2004.

[15] A. P. Dowling and S. R. Stow, “Acoustic analysis of gas-turbine combustors,” in *Combustion instabilities in gas turbine engines: operational experience, fundamental mechanics, and modeling*, Raston -USA: American Intstitute of Aeronautics and Astronautics, Inc., (2005), pp. 369–414.

[16] X. Han and A. S. Morgans, “Simulation of the flame describing function of a turbulent premixed flame using an open-source LES solver,” *Combust. Flame*, vol. 162, no. 5, (2015) pp. 1778–1792.

[17] J. Li, D. Yang, C. Luzzato, and A. S. Morgans, “Open Sounce Combustion Instability Low Order Simulator (OSCILOS--Long) Technical report,” London, 2015.

[18] G.-M. Choi and M. Katsuki, “Advanced low NOx combustion using highly preheated air,” *Energy Convers. Manag.*, vol. 42, no. 5, (2001) pp. 639–652.

[19] P. Jansohn, T. Griffin, I. Mantzaras, F. Marechal, and F. Clemens, “Technologies for gas turbine power generation with CO2 mitigation,” in *Energy Procedia*, 2011.

[20] P. E. Røkke and J. E. Hustad, “Exhaust gas recirculation in gas turbines for reduction of CO2 emissions; combustion testing with focus on stability and emissions,” *Int. J. Thermodyn.*, vol. 8, no. 4, (2005) pp. 167–173.

[21] “UKCCSRC, Gas turbine with exhaust gas recycle – Pilot-scale advanced capture technology,” 2013. [Online]. Available: http://www.pact.ac.uk/facilities/PACT-Core-Facilities/Gas-Turbine/gas-turbine-with-exhaust-gas-recycle-gt-egr/.

[22] “UKCCSRC.” [Online]. Available: WWW.pact.ac.uk/facilities/PACT-Core-Facilities/Gas-Turbine/gas-turbine-with-exhust-gas-recycle-gt-egr. [Accessed: 10-Oct-2016].

[23] E. R. Earnest, “Turbine engine with exhaust gas recirculation.” Google Patents, 1981.

[24] H. Li, G. Haugen, M. Ditaranto, D. Berstad, and K. Jordal, “Impacts of exhaust gas recirculation (EGR) on the natural gas combined cycle integrated with chemical absorption CO 2 capture technology,” *Energy Procedia*, vol. 4, (2011) pp. 1411–1418.